Impacts of demand response from buildings and centralized thermal energy storage on district heating systems

Sustainable Cities and Society 64 (2021) 102510

Contents lists available at ScienceDirect

Sustainable Cities and Society

journal homepage: www.elsevier.com/locate/scs

Impacts of demand response from buildings and centralized thermal energy storage on district heating systems

Dmytro Romanchenko *, Emil Nyholm, Mikael Odenberger, Filip Johnsson

Department of Space, Earth and Environment, Chalmers University of Technology, S412 96 Göteborg, Sweden

ARTICLE INFO

Keywords:
District heating
Space heating demand
Demand response
Thermal energy storage
Optimization
Modeling

ABSTRACT

Energy use for space heating is a substantial part of total energy end use and heating systems can offer some flexibility in time of use, which should be important in future energy systems to maintain balance between supply and demand. This work applies a techno-economic, integrated, demand-supply optimization model to investigate the combined effect of using demand-side flexibility from buildings, by allowing for indoor temperature deviations (both up- and downward from the set-point), and supply-side flexibility, by applying thermal energy storage (TES), on the operation of district heating (DH) systems.

The results indicate that the potential for increased indoor temperature, i.e., demand response (DR), is concentrated to multi-family and non-residential buildings (heavy buildings with high time-constants), while the potential for downregulation of the temperature, i.e., operational energy savings, is utilized to a greater extent by single-family buildings (light buildings). It is also evident that the value of DR diminishes in the presence of a supply-side TES. We show that applying both the demand-side flexibility and a centralized TES is complementary from the heating system perspective in that it results in the lowest total space heating load of the buildings and the lowest running cost for the DH system.

1. Introduction

Flexibility in thermal networks, i.e., district heating (DH) and cooling systems, has been suggested as an important way to facilitate the use of high levels of renewable energy resources in the energy system (Lund, Lindgren, Mikkola, & Salpakari, 2015; Paiho et al., 2018). Flexibility in such systems can be provided by thermal energy storage (TES) in the form of the thermal inertia of buildings, heat storage units, and the DH network itself. Studies have investigated the effects of centralized TES tanks on the operation of DH systems (e.g., Bachmaier, Narmsara, Eggers, & Herkel, 2016; Buoro, Pinamonti, & Reini, 2014; Li, Rezgui, & Kubicki, 2020; Oluleye, Vasquez, Smith, & Jobson, 2016) and other studies have examined the effects of the space heating demand response (DR) in buildings, i.e., the utilization of the thermal inertia of buildings as TES, on the operation of DH systems (e.g., Cai et al., 2018; Ingvarson & Werner, 2008; Kensby, Trüschel, & Dalenbäck, 2015; Li & Wang, 2015). All these studies concluded that availability of a TES benefits operation of energy systems, e.g., by reduced running costs or allowing greater shares of variable renewable energy sources such as wind and solar power. Nevertheless, studies that compare the effects of centralized TESs and DR in buildings on the operation of DH systems are lacking.

A previous study conducted by the authors Romanchenko, Kensby, Odenberger, and Johnsson (2018) compared the utilization patterns and the effects of TES in the form of thermal inertia of buildings, i.e., DR in buildings achieved via upward indoor temperature deviations, and a centralized TES tank, on the operation of the DH system of Gothenburg, Sweden. Romanchenko et al. (2018) concluded that the TES in buildings and the TES tank benefit the operation of the DH system and have similar dynamics of utilization, although only the centralized TES is used for storing energy for periods longer than days owing to the incurring of lower energy losses compared to DR. However, in that study, the effects of TES on the operation of the DH system were investigated by applying the storage types one at a time and the study was limited to the present building stock and DH supply system, which is also true for most of the other published works on this topic. The study of Verrilli et al. (2017) focused on the design of a model predictive controller, with the aim of reducing the operating and maintenance costs of a DH system with installed TES and "flexible loads" (i.e., reschedulable and curtailable loads). The study of Dominković, Gianniou, Münster, Heller, & Rode (2018) applied a two-level modeling approach,

* Corresponding author.
E-mail address: dmytror@chalmers.se (D. Romanchenko).

https://doi.org/10.1016/j.scs.2020.102510
Received 4 July 2020; Received in revised form 20 September 2020; Accepted 21 September 2020
Available online 29 September 2020

whereby the results from a building simulation model were fed into a linear energy system optimization model (including the power, heating, gas and transport sectors), with the aim of studying the DR potential of existing Danish single-family residential buildings connected to a DH system. The modeling methods applied in the abovementioned two studies (Dominković et al., 2018; Verrilli et al., 2017) allow for optimization of the operation of DH systems through considering a centralized TES and activation of DR in combination (applied at the same time), and both studies have reported complementary positive effects of a TES and DR on the efficiency of the heat supply in DH systems. Yet, the "flexible loads" described by Verrilli et al. (2017)) are not explicitly related to the DR in buildings and, therefore, provide no information on how these loads influence the energy demand profile and the overall flexibility potential of the buildings. In the study of Dominković et al. (2018), the flexibility potential of buildings for the energy system was pre-calculated in a building simulation model by running a 1-day simulation that consisted of the following three phases: 1) pre-heating of buildings; 2) a cutoff period, during which the heat supply to buildings is assumed to be turned off; and 3) heating after the cutoff period. Thus, this limits the flexibility potential of buildings to a simulated (pre-defined) DR profile and does not account for the feedback mechanism between supply and demand, e.g., the effects of changed space heating demand from buildings on the heat generation in DH systems.

To date, most of the research studies have investigated either the effects of a centralized TES or the effect of DR on the operation of DH systems, and thus do not provide any insights into whether centralized TES and DR in buildings are complementary or competing within DH systems. The studies that investigated TES and DR simultaneously in DH systems were not able to capture the demand- and supply-side feedback mechanism (Dominković et al., 2018; Verrilli et al., 2017). The method developed and applied in this work is novel and relies on an integrated demand-supply optimization model, which allows for concurrent optimization of space heating demand in buildings, including the possibility to vary the indoor temperature, and heat generation in a DH system with available centralized TES. Thus, our method allows for competition between decentralized (DR in buildings) and centralized (TES) flexibility measures in DH systems, which is deemed novel in the research field, by minimizing the variable cost of heat generation from the societal perspective. Furthermore, the value of operational energy savings derived from allowing indoor temperature deviations below the set-point value in buildings is investigated in this work. Another contribution of this work is that the model is applied to the Building Stock (BS) and the DH system projected to Year 2050 (of Gothenburg, Sweden), as compared to the aforementioned works, which are focused on current BSs and DH systems.

The main research questions addressed in the present work are:

1) In what ways do the indoor temperature and space heating demand in buildings change when one allows for flexibility in buildings through temperature deviations from the set-point value? In what respects does this depend on the building type and DH system set up (with/without a centralized TES)?
2) How does the total system (city's) heating load change and what are the benefits derived by a DH system, from the activation of energy flexibility in buildings or utilization of a centralized TES and these two actions combined?

This paper is organized as follows: Section 2 outlines the modeling approach applied and the DH system and associated building stock investigated together with the modeling scenarios, while Section 3 describes and discusses the results obtained from the modeling, Section 4 summarizes the conclusions drawn from the study.

2. Methodology

The optimization modeling integrates the calculation of the space heating demand in buildings and the heat generation and storage in a DH system within a single framework, thereby enabling the abovementioned feedback mechanism between demand and supply – a novel aspect of the present work. This feature allows for investigation of the reciprocal effects of flexible operation of buildings and DH systems with and without a centralized TES. Furthermore, allowing for both upward and downward regulation of the temperature in buildings provides the possibility to investigate and compare the effects of DR and operational energy savings on the energy behaviors of buildings and on the total system (city's) heating load. The investigated BS and DH systems are assumed to be representative of Year 2050.

2.1. Modeling approach

The model is a techno-economic, mixed-integer, Energy Balance Unit Commitment (EBUC) optimization model that integrates a physical space heating demand model of a BS with a dynamic unit commitment model of a DH system. The EBUC model was developed, validated against measured data and described in detail in a previous study conducted by the authors (see Romanchenko, Nyholm, Odenberger, & Johnsson, 2019)* . In this work, the original EBUC model is further developed to include a description of a centralized TES. The objective function of the model is to find the least-cost dispatch, i.e., total running cost (which comprises fuel costs, operation and maintenance costs and fuel and carbon taxes), of the DH system while maintaining the energy balance between demand and supply. The EBUC model has a temporal resolution of 1 hour, and the optimization is carried out with a time horizon of 1 year and with perfect foresight.

The total system heating demand, which is met by the heat generation units available in the DH system, is here assumed to consist of the space heating demand from buildings and the "non-space" heating demand. The space heating demand from buildings is endogenously calculated in the EBUC model and includes the energy flexibility from buildings conferred by either activating only DR, which in this work is achieved through upward indoor temperature deviations, or activating DR together with the operational energy savings potential, i.e., achieved through downward temperature deviations. As a result, the space heating demand in the buildings can be shifted in time as long as the indoor temperature stays within the pre-defined temperature range. The non-space heating demand (e.g., hot water demand from buildings and/or demand from industrial users) is assumed to be inflexible and is given to the model exogenously.

So-called representative buildings are used to describe the BS modeled in the EBUC model. The space heating demand from the representative buildings is calculated using an energy balance over each modeled building while considering two thermal zones: 1) an external thermal zone, which represents the building envelope; and 2) an internal thermal zone, which represents the indoor air, furniture, and outer layers of the internal walls. The calculated space heating demand of each modeled building is then extrapolated to represent the overall space heating demand of the BS using building stock weight coefficients. The calculations of the space heating demand over the modeled BS and the non-space heating demand are described in more detail elsewhere (Romanchenko et al., 2019). The authors have previously described (Romanchenko, Odenberger, Göransson, & Johnsson, 2017, 2018) the EBUC least-cost unit commitment and dispatch modeling of the heat generation and storage units available in the DH system.

* See Supplementary Materials for the model formulation in the modeling syntax GAMS (GAMS.com, 2015).

2.2. Case study

The BS and the DH system of Gothenburg, Sweden projected to Year 2050 are used as a case study in this work and are described as follows.

2.2.1. Building stock

In the EBUC model, 134 representative buildings, including residential and non-residential buildings, represent the BS of Gothenburg. To describe the BS of Gothenburg in Year 2050, the following assumptions are made: 1) the buildings connected to the DH system in Year 2050 are the same as those in Year 2012 (in this work, all the data not projected to Year 2050 come from Year 2012); and, 2) the properties of the representative buildings in Year 2050 are the same as those in Year 2012, except for the data on U-values and the availability of a ventilation heat recovery (VHR) system in buildings, which are obtained as described below. The input data describing the BS are mainly based on the BETSI study conducted by the Swedish National Board of Housing Building and Planning (The National Board of Housing, 2010). The BETSI database contains detailed descriptions of 1,800 existing buildings, which were chosen as being representative of the standing Swedish BS in Year 2005. Additional archetype buildings were created to represent the buildings constructed during the period2005–2012. How the representative buildings and their respective weight coefficients were chosen is explained in greater detail in the previous work by the authors (Romanchenko et al., 2019). The parameters that describe the representative buildings in the EBUC model are listed in Table A1 in Appendix A.

As mentioned above, in this work, the assumption is made that the representative buildings develop until Year 2050 (relative to Year 2012) with respect to improvements in thermal energy performance, which are achieved through lowering the U-value of the buildings and/or by installing a VHR system. The data describing the U-values and the availability of a VHR system in the representative buildings in this work are based on the previous work of the authors, which applied investment modeling to study the development scenarios of the BS and DH system of Gothenburg up to Year 2050 (Romanchenko, Nyholm, Odenberger, & Johnsson, 2020). That work includes the development scenario, which should reflect the EU's building renovation rates estimated to comply with the climate targets and in which the total space heating demand from the BS of Gothenburg is reduced by 60% by Year 2050, as compared to Year 2020. The information on the U-values and the availability of VHR systems in the representative buildings in Year 2050 is extracted from that scenario and exogenously applied to the EBUC model (in all the investigated scenarios described in Section 2) in this work. Hence, it can be stressed again that the description of the investigated BS in Year 2050 differs from its description as of Year 2012 in regard to U-values of the building envelope components and the availability of a VHR system. The applied U-values of the representative buildings are shown in Fig. A1 in Appendix A. All the representative buildings are modeled with installed VHR systems.

2.2.2. District heating system

The descriptions of the heat generation and storage units available in the DH system of Gothenburg in Year 2050 are also based on the previous work conducted by the authors, which applied investment modeling to study the development scenarios of the BS and DH system of Gothenburg (Romanchenko et al., 2020). Hence, in the present work, the DH system is assumed to comprise a source of industrial waste heat (e.g., a biorefinery), a municipal waste incineration plant, two industrial heat pumps (HPs) (one using sewage water as the heat source and one using outside air), an electric boiler, and a seasonal pit TES (although, the pit TES is assumed to be available in the DH system only in the scenarios "with TES", which are described in detail in Section 2.3). Assumptions regarding the technical and economic parameters describing the heat generation units and the pit TES are given in Tables A2 and A3, respectively, in Appendix A. The coefficient of performance (COP) values of the HPs are assumed to be variable. The COP for each time-step (hour) is treated as a function of the temperature profiles of the available heat sources, i.e., sewage or outdoor air, and the heat sink, i.e., the DH system supply water. The hourly values for the supply and return water temperatures in the DH network were provided by the DH system operator. The energy losses in the DH heat exchangers (substations) in buildings are assumed to be 10%. Interconnections of the modeled DH system with the neighboring DH systems of other municipalities are not modeled in this work, mainly because of the comparatively low levels of exchanged heating energy.

Table 1
The distinguishing features of the six scenarios investigated in this work. A cross indicates the availability of a feature in the scenario, while a minus sign indicates the absence of a feature.

Scenario name	**Upward** temperature deviations	**Both** upward and downward temperature deviations	**TES**
Ref.	-	-	-
T_{up}	×	-	-
T_{both}	×	×	-
TES	-	-	×
TES_ T_{up}	×	-	×
TES_ T_{both}	×	×	×

2.2.3. Other input data

The hourly outdoor air and ground temperatures are provided by the DH system operator for Year 2012. The solar irradiation data for the same year are obtained from the Swedish Meteorological and Hydrological Institute (SMHI) (SMHI—Swedish Meteorological & Hydrological Institute, 2017). The temperature profiles and the solar irradiation data are used for the model year 2050. The hourly electricity prices for Year 2050 are extracted from the ELIN/EPOD modeling package (Göransson, Goop, Unger, Odenberger, & Johnsson, 2014; Odenberger, Unger, & Johnsson, 2009), which also uses weather data from Year 2012 as reference. The data for Year 2012 is the most recent data with matching hourly profiles of outdoor temperature, solar irradiation, heating load and electricity prices, which is important when studying the effects of DR and TES on energy systems, as is the case in this work. The non-space heating demand and the DH network energy losses are described elsewhere (Romanchenko et al., 2019), and they are exogenously included in this work as a single demand profile.

2.3. Scenarios

Six scenarios are used to study the interplay between the energy use in buildings, with and without activated energy flexibility, and the DH system with and without the presence of a central TES. In the Reference (*Ref.*) scenario, no active DR is allowed in the investigated buildings, i.e., the space heating demand is calculated with the objective of maintaining the indoor air temperature in the buildings at a set-point value. However, the indoor air temperature is not prevented from increasing above the set-point value due to the influences of, for example, the outdoor air temperature, solar irradiation, and internal heat gains. In the T_{up} scenario, upward indoor temperature deviations due to active DR are

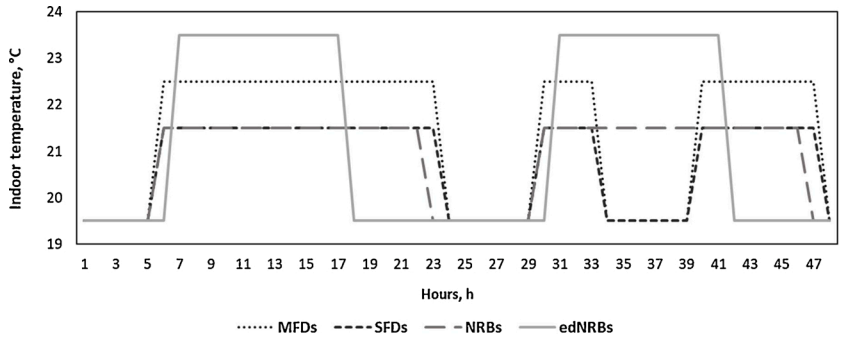

Fig. 1. The lower boundaries of the allowed indoor air temperature deviations in the building types included in the modeling of this work: MFDs, SFDs, NRBs, and edNRBs, illustrated for a 2-day period (weekend and weekday) and for the scenarios with allowed downward temperature deviations, i.e., T_{both} and TES_T_{both}.

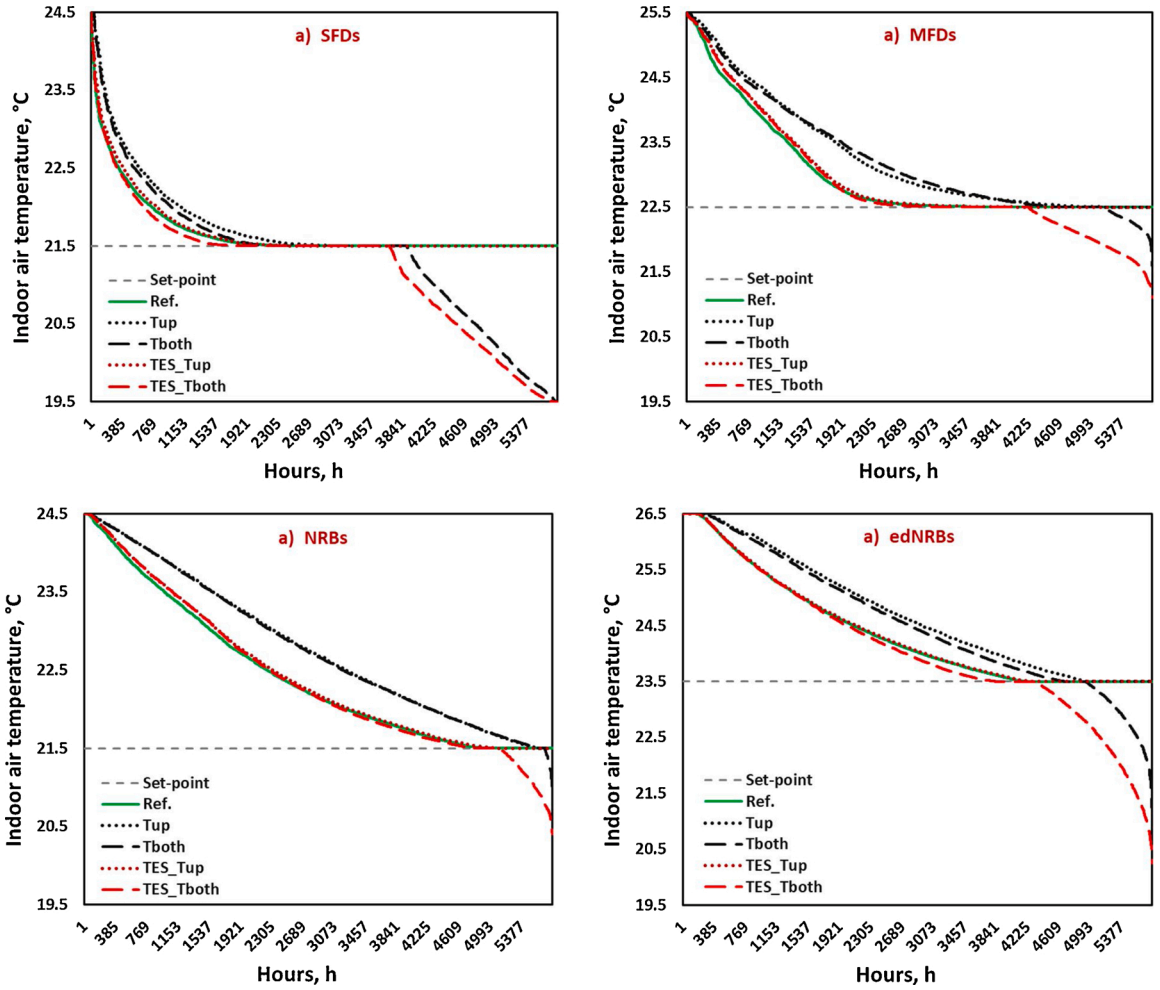

Fig. 2. The hourly values of the indoor air temperature averaged over the representative: (a) SFDs, (b) MFDs, (c) NRBs, and (d) edNRBs, and sorted in descending order, as obtained through the EBUC modeling in the *Ref.*, T_{up}, T_{both}, TES_T_{up}, *and* TES_T_{both} scenarios (the temperatures in the *TES* scenario are identical to the temperatures in the *Ref.* scenario and, hence, are not presented). The bounds of the *y*-axes are adjusted to the values of the lowest (19.5 °C) and the highest (e.g., for SFDs, 24.5 °C) allowed indoor air temperature in each of the building types. The *x*-axes are limited to 5,759 hours because the period from May 15th to September 15th is excluded. The dashed gray lines represent the set-point temperature values assumed for the building types.

allowed, while downregulation of the indoor temperature is not allowed. Here, active DR is associated with periods of supplying more heating energy from the DH network than is required by the buildings, i.e., compared to the demand in the *Ref.* scenario, followed by periods of supplying less heating energy than is required by the buildings. In the T_{both} scenario, both upward and downward deviations of the indoor temperature are allowed, i.e., the effects of DR and operational energy savings on the energy behaviors of buildings and on the total system (city's) heating load are investigated. In the *Ref.*, T_{up}, *and* T_{both} scenarios, it is assumed that there is no centralized TES available within the DH system. The *TES*, TES_T_{up}, and TES_T_{both} scenarios are almost identical to the *Ref.*, T_{up}, *and* T_{both} scenarios, respectively, with the only difference being that a pit TES is now available in the DH system. Table 1 lists the factors that distinguish the six scenarios in terms of the allowed

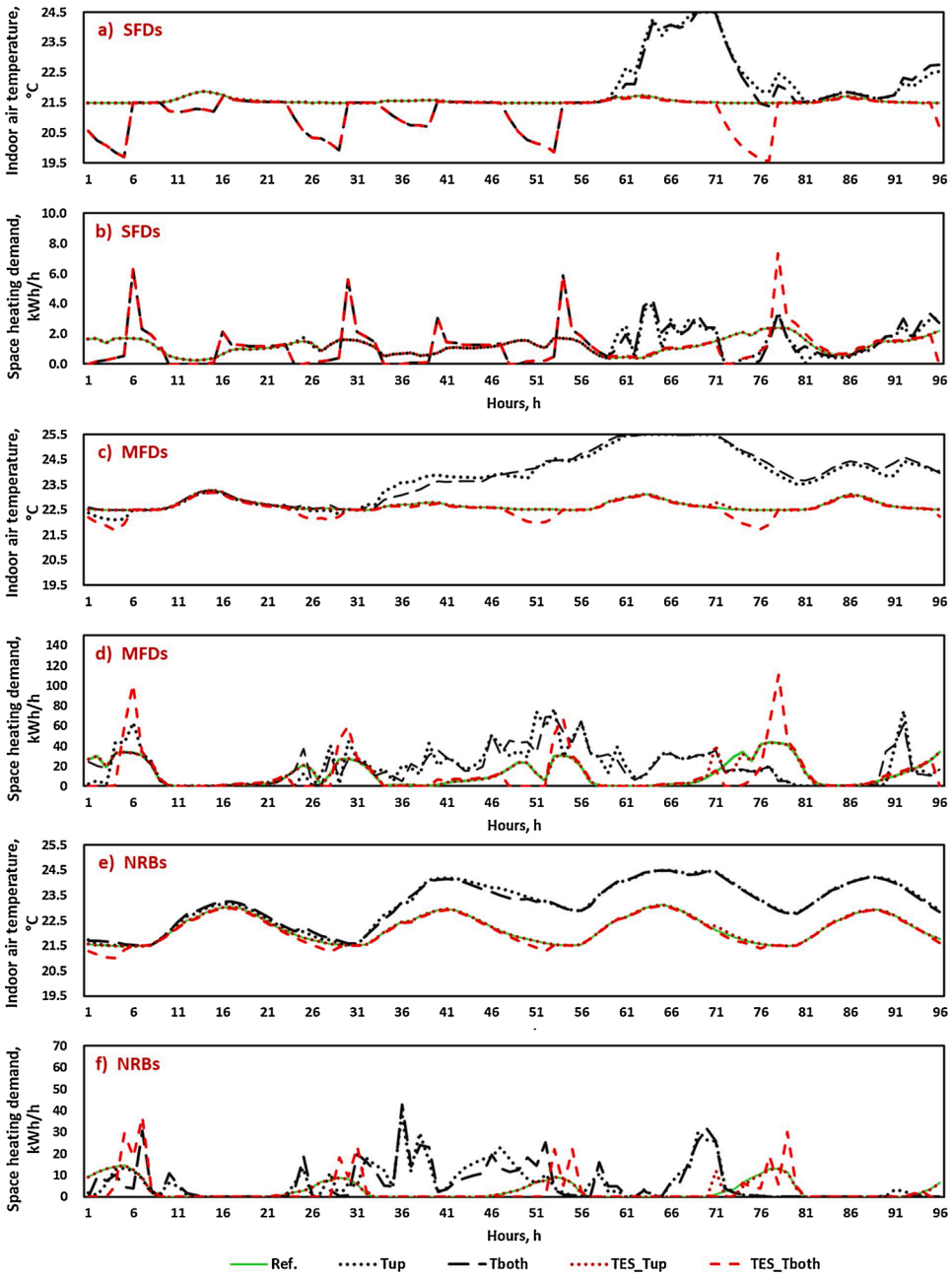

Fig. 3. The hourly indoor air temperatures averaged over the representative: (a) SFDs, (c) MFDs, and (e) NRBs, and hourly space heating demands averaged over the representative (b) SFDs, (d) MFDs, and (f) NRBs, as obtained through the EBUC modeling in the *Ref.*, T_{up}, T_{both}, *TES*_T_{up}, *and TES*_T_{both} scenarios (the values in the *TES* scenario are identical to the values in the *Ref.* scenario and, hence, are not presented) and shown for 4 days in February. The boundaries of the *y*-axes in (a), (c), and (e) are adjusted to the values of the lowest (19.5 °C) and the highest (e.g., for SFDs, 24.5 °C) allowed indoor air temperature in the buildings. The bounds of the y-axes in (b), (d), and (f) are adjusted to the highest presented average space heating demand in the SFDs, MFDs, and NRBs, respectively.

Table 2
Total number of hours and standard deviation of the amplitude of the events during which the total space heating load of the city (all the modelled buildings) increased or decreased in each of the T_{up}, T_{both}, TES_T_{up}, and TES_T_{both} scenarios, as compared to the *Ref.* scenario.

		T_{up} *vs Ref.*	T_{both} *vs Ref.*	TES_T_{up} *vs Ref.*	TES_T_{both} *vs Ref.*
Total number of hours*, (h)	*increased***	2,042	2,630	**532**	2,828
	*decreased***	2,552	2,504	**900**	2,361
Standard deviation of the amplitude (MWh/h)	*increased*	35.6	35.7	15.8	**62.2**
	decreased	27.1	31.6	10.1	**53.5**

* Note that the maximal number of hours available for the increase or decrease in the load is 5,759.
** Only the hours during which the total space heating load was increased or decreased by ≥1 MWh/h are included.

temperature deviations and whether or not the TES is included.

The indoor air set-point temperatures in multi-family dwellings (MFDs), single-family dwellings (SFDs), and non-residential buildings (NRBs) are set at 22.5 °C, 21.5 °C, and 21.5 °C (23.5 °C in educational buildings – denoted edNRBs), respectively (Grundsell, 2013; Langer & Bekö, 2013; Socialstyrelsen, 2005). The indoor air temperature in the representative buildings can deviate upwards from the respective set-point temperatures by up to 3 °C (indoor temperature deviations greater than +3 °C are prevented in all the scenarios), which is within the recommended indoor temperature comfort range for living spaces, according to ISO Standard for Ergonomics of the Thermal Environment (ISO, 2005), and for office environments, according to American Society of Heating and Refrigerating and Air Conditioning Engineers (ASHRAE) (summarized in (GÜNGÖR, 2015)).

In the T_{both} and TES_T_{both} scenarios, the indoor air temperature in the buildings can deviate upwards by up to 3 °C from the set-point value as well as downwards according to a pre-defined profile. Fig. 1 shows the lower boundaries of the allowed indoor air temperature deviations in the building types in the T_{both} and TES_T_{both} scenarios. It is assumed in this work that all the building types can decrease in temperature during night-time, while only the SFDs and MFDs can reduce their indoor air temperatures to 19.5 °C (based on the information provided in Langer & Bekö (2013) and Socialstyrelsen, (2005)) during daytime on workdays.

It is assumed that the space heating demand from the investigated BS is zero during the period of May 15th – September 15th.

3. Results and Discussion

3.1. Changes in the indoor temperature and space heating demand profile of buildings

The modeling results show that the DR in the buildings, in terms of indoor temperature changes, depend on the building type and whether or not a centralized TES is available within the DH system. Fig. 2 shows the duration of the indoor air temperature, i.e., the hourly temperature values sorted in descending order, averaged over the representative building types of SFDs, MFDs, NRBs, and edNRBs, as obtained from the modeling. The results show that the potential of upregulation of the indoor temperature (active DR) is utilized to a greater extent by the MFDs and NRBs, while the potential of downregulation (operational energy savings) is utilized to a greater extent by the SFDs. The average yearly indoor air temperatures in the SFDs in the T_{both} and TES_T_{both} scenarios are 21.4 °C and 21.2 °C, respectively, as compared to 21.7 °C in the *Ref.* scenario. The average yearly indoor air temperatures in the MFDs in the T_{up} and T_{both} scenarios (scenarios without TES) are higher than in the *Ref.* scenario by 0.3 °C and 0.2 °C, respectively. The temperature differences in the NRBs between the same scenarios are even larger (the yearly average indoor air temperatures of the representative SFDs, MFDs, and NRBs individually are shown in Fig. B1, Appendix B). These results can be explained by the fact that the MFDs and NRBs have greater thermal capacities (time constants) than the SFDs and, therefore, greater potential for storing energy. The SFDs, owing to their lighter structures and higher surface area-to-volume ratios, are more suitable for exploiting the potential to decrease the indoor air temperature so as to reduce the total space heating demand. The reason the potential for downregulation of the indoor temperature is not fully utilized by the buildings, especially the MFDs and NRBs, is to a large extent related to the limitations on the time and magnitude of the downregulation (*cf.* Fig. 1). Therefore, if there was no requirement to restore the indoor temperature every 6 hours (as required now), the MFDs and NRBs could have utilized the operational energy savings potential via downregulation of the temperate to a greater extent.

It should be noted that the average yearly indoor air temperatures in all the building types are higher in the *Ref.* scenario than the respective set-point values. This is due to optimal utilization of heat gains, i.e., the indoor temperature in buildings exceeds the set-point value due to the combined effect of solar irradiation, outdoor temperature, and indoor activities. It should also be kept in mind that the BS modeled is an approximation of the BS in Year 2050, and thus, it has significantly improved energy performance in terms of U-values and VHR. The results show that the average hourly indoor air temperature in the NRBs remains above the set-point value of 21.5 °C for 4,849 hours, out of the total considered 5,759 hours, due to the optimal utilization of heat gains already in the *Ref.* scenario. In the T_{up} and T_{both} scenarios, this number increases to 5,555 hours. This indicates that by Year 2050 the modeled buildings are close to becoming passive houses in terms of energy utilization.

Fig. 2 also shows that the hourly values of the average indoor air temperature in each investigated building type are higher in the scenarios without TES (T_{up} and T_{both} scenarios – black lines) than in the corresponding scenarios with TES (TES_T_{up} and TES_T_{both} scenarios – red lines) in the DH system. However, the extent to which the indoor air temperature differs between the scenarios with and without the TES depends on the building type. For SFDs, both the increases and decreases in the indoor temperature in all the scenarios follow each other closely, albeit with marginally smaller upward temperature deviations and marginally larger downward temperature deviations in the scenarios with TES. For the MFDs and NRBs, the effects of the TES on both the upward and downward temperature deviations are stronger. The scenarios with TES show both smaller increases in temperature (on average by 0.3 °C) and fewer hours with increased temperature compared to the scenarios without TES. Regarding downregulation of the indoor temperature, the scenarios with TES show larger decreases in temperature and higher numbers of hours with decreased temperature, For example, in the case of the NRBs, the number of hours with downregulation in the T_{both} scenario is just less than 100, while for the TES_T_{both} scenario the

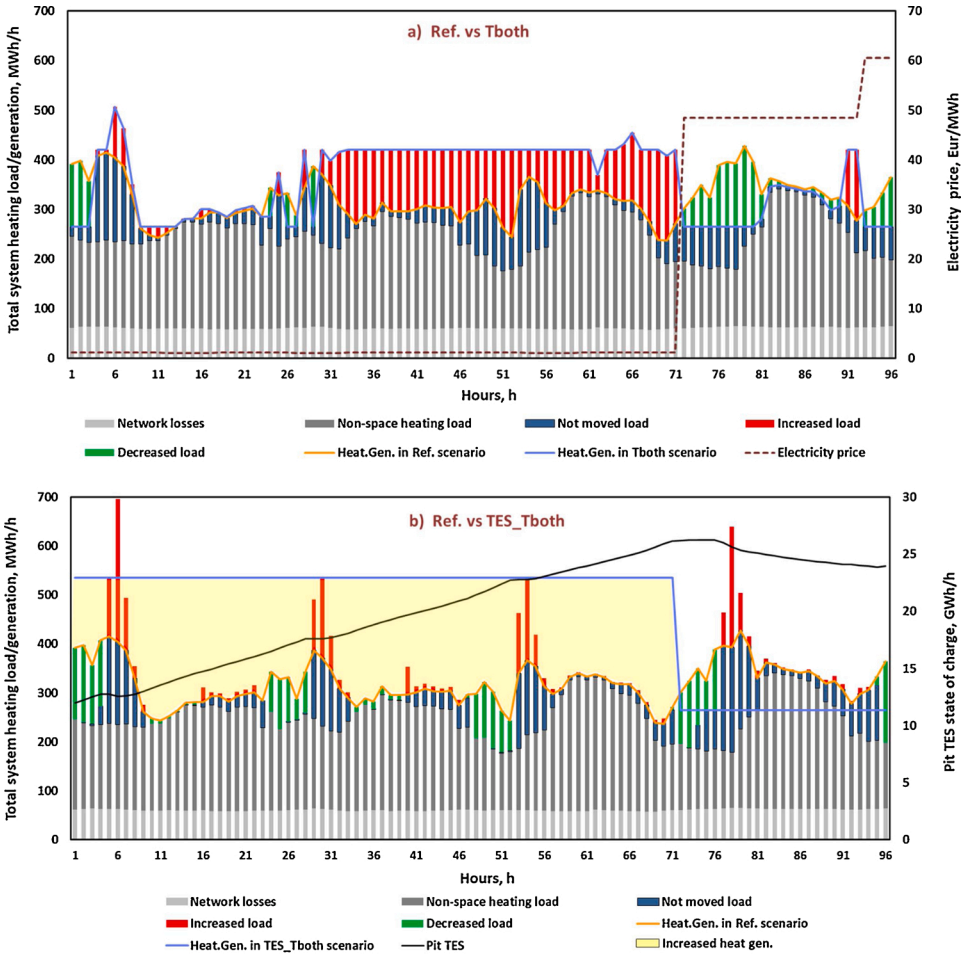

Fig. 4. The total system heating demand, divided into network losses, non-space heating load, and *not moved*, *increased*, and *decreased* space heating load in the (a) T_{both}, and (b) *TES_*T_{both} scenarios, as compared to the *Ref.* scenario, presented for 4 days in February, together with the total system heat generation in the *Ref.*, T_{both}, and *TES_*T_{both} scenarios, the electricity price (a) and the state of charge for the TES (in the *TES_*T_{both} scenario) (b). The light-yellow area in b) highlights the difference between the total system heat generation and the total system heating load, which reflects the heating energy charged to the TES or covering for the peaks (red bars) in the total system heating load, in the *TES_*T_{both} scenario.

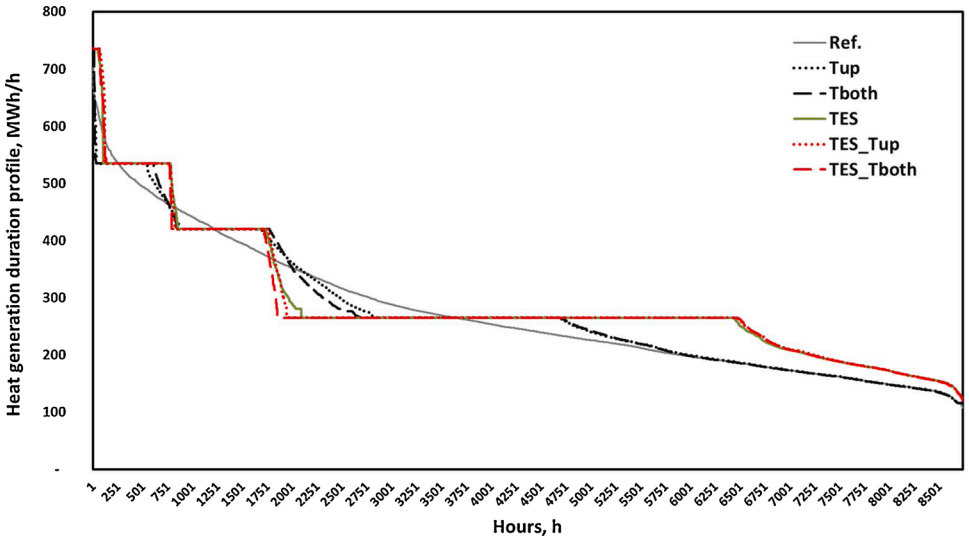

Fig. 5. The heat generation profiles, sorted in descending order, for the investigated DH system of Gothenburg, as obtained through the EBUC modeling for the six investigated scenarios.

corresponding number of hours is 650 (note that the maximal number of hours available for downregulation in all the buildings is limited by the profiles shown in Fig. 1). These results indicate that the availability of a centralized TES in the DH system alleviates the need for upregulation of the indoor temperature, in that the economic gains from smoothening the dispatch in the DH system can be achieved by the TES. Moreover, the presence of the TES makes it possible to use more downregulation of the indoor temperature to achieve additional energy savings in all the building types (even more economic gains). Thus, DR in buildings can function either to harmonize fluctuations for the supply system or as a means to reduce energy use, and the optimal combination will depend on the availability and dimensioning of the centralized TES and the supply units themselves.

Fig. 3 shows the hourly indoor air temperatures and corresponding space heating demands in the representative SFDs, MFDs, and NRBs, as obtained from the modeling for 4 days in February. The results show that the largest changes in space heating demand are caused by the downregulation of the indoor temperature in the *TES_T$_{both}$* scenario. In that scenario, new peaks in the space heating demand are created as the indoor temperature, which was lowered during the periods of allowed downregulation, needs to be recovered. The results show that the largest dips in the indoor temperature, down to the lowest allowed temperature of 19.5 °C, occur in the SFDs and result in the new space heating demand peaks being up to 3.5-times higher (average for SFDs) than the demand peaks in the *Ref.* scenario. The results show that even though the downregulation of the temperature in the *TES_T$_{both}$* scenario results in new, significantly higher short-term peaks in the space heating demand, the total space heating demand from buildings is reduced, which is

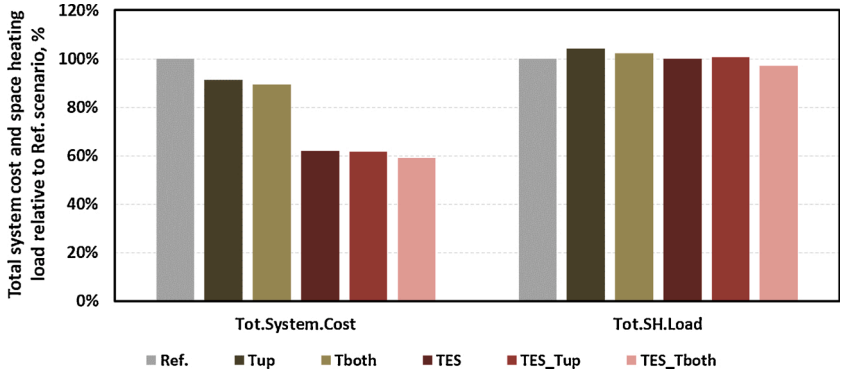

Fig. 6. Changes in the total yearly running cost and the total yearly space heating load supplied by the DH system, as obtained from the modeling of the *T$_{up}$*, *T$_{both}$*, *TES*, *TES_T$_{up}$*, *and TES_T$_{both}$* scenarios. Presented are the percentages relative to the 100% assigned to the *Ref.* scenario.

beneficial from the system perspective. Nevertheless, such large and short-term peaks in demand pose significant challenges for the dispatch of the heat generation and storage units and the operation of the DH substations and heat exchangers in the buildings. The results show that the capacity and coordinated operation of the heat generation and storage units can satisfy such peaks in the demand (further explained in Section 3.2). From the DH network perspective, comparing the maximal values of the space heating demand peaks in the buildings and the total system heating load of the city in the studied Year 2050 to the respective values in Year 2012, it can be concluded that the capacity of the DH substations and heat exchangers is sufficient to manage the observed demand variations. This is under the condition that the capacity of the heat exchangers is not decreased in the future.

Fig. 3 also shows that the strongest upregulations of the temperature occur in the T_{up} and T_{both} scenarios. The average indoor air temperatures in the MFDs and NRBs remain above the respective set-point values for a couple of days (between Hours 33 and 96). Fig. 3b shows that the space heating demand from the MFDs between Hours 33 and 71 is higher in the T_{up} and T_{both} scenarios, as compared to the *Ref.* scenario. This indicates that the increase in the indoor temperature in the MFDs during these hours is due to active DR. This behavior of the buildings is driven by the requirement to optimize the heat generation in the DH system in the absence of the pit TES, which is explained in Section 3.2.

3.2. The effects of flexibility on the total system heating load and the operation of the DH system

The modeling results show that the total system heating load changes, in terms of shifted energy, in different ways with the allowed DR and operational energy savings in buildings and in the presence and absence of a centralized TES. Table 2 shows the total number of hours and standard deviation of the amplitude of the events during which the total space heating load of the building stock increased or decreased in each of the T_{up}, T_{both}, *TES*_T_{up}, and *TES*_T_{both} scenarios, as compared to the *Ref.* scenario. Table 2 shows that the T_{up} and T_{both} scenarios are similar in terms of both indicators, indicating a weak effect of the potential to downregulate the temperature in buildings on the total space heating load in the scenarios in which centralized TES is not available. This is likely because the potential for the downregulation of the indoor temperature is mainly exploited in the T_{both} scenario by the SFDs, which constitute a comparatively small part of the total system heating load, as compared to the MFDs and NRBs, and therefore they have a weak effect on the load shifting. It is also noteworthy that the events of increased and decreased space heating load are the lowest in number as well as amplitude in the *TES*_T_{up} scenario, which supports the notion that the availability of TES in the DH system reduces the need to use the buildings for DR. The *TES*_T_{both} scenario shows similar values in terms of the total number of hours of the events of increased and decreased total space heating load to the T_{up} and T_{both} scenarios, albeit with noticeably higher values for the standard deviation of the amplitude of the increases and decreases. This is due to the high number of large, short-terms peaks in the space heating demand from buildings, associated with the downregulation of the temperature, which is further explained below and shown in Fig. 4b.

To illustrate how the shifted energy affects the total system heating load profile, Fig. 4 shows the modeled heating load curves for 4 days in February in the T_{both} and *TES*_T_{both} scenarios. The modeled heating load curves are divided into network losses, non-space heating load (hot-water demand from buildings and demand from industrial users), and space heating load from the buildings shown as *not moved*, *increased*, or *decreased* in the T_{both} and *TES*_T_{both} scenarios, as compared to the *Ref.* scenario. Fig. 4a exemplifies one of the DR events (i.e., active overheating of buildings is followed by underheating), during which the upregulation of the temperature in the buildings is activated in response to a "signal", in this case the change in the electricity price, with the objective of optimizing the heat generation in the DH system. During Hours 33–71 in Fig. 4a (hours with low electricity prices), the total system load in the T_{both} scenario is larger than in the *Ref.* scenario at 420 MW h/h, which corresponds to the maximum total heat outputs from the base-load waste-based heat generation units and the sewage water-based HP, for the majority of the hours. During these hours, the heating energy is accumulated in the buildings and, therefore, allows for reduced space heating load during Hours 72–90, a period that is characterized by significantly higher electricity prices. This, in turn, results in a decreased output of the sewage water-based HP during these hours and, correspondingly, a reduced cost for heat generation.

Fig. 4b presents the energy shifting pattern that is distinctive for the *TES*_T_{both} scenario and occurs due to the combined effect of the allowed downregulation of the temperature in buildings and the availability of TES in the DH system. In this pattern, the space heating load first decreases due to the allowed downregulation of the temperature, and thereafter drastically increases to restore the indoor temperature in the buildings (i.e., the opposite to the pattern of active DR, during which a decrease in the load follows the increase). Interestingly, this pattern is merely observed in the T_{both} scenario, indicating the importance of the TES (i.e., the extra capacity that the TES provides) for it to occur. Fig. 4b shows that during the peaks in the total system heating load in the *TES*_T_{both} scenario (around Hours 6, 30, and 55), the state of charge of the TES stays constant or slightly decreases (discharges), while the level of heat generation is higher than in the *Ref.* scenario. This indicates that the heating energy generated in the DH system is not stored in the TES but is instead being used to compensate for the peaks in the space heating load. Otherwise, during almost the entire period spanning Hours 1-71, the heat generation in the *TES*_T_{both} scenario is greater than that in the *Ref.* scenario, with the TES being charged. During Hours 72–96, the opposite situation prevails. This clearly shows the dynamics of maximizing the output of the heat generation units, in this case HPs, during the periods with low fuel/electricity prices (*cf.* Fig. 4a for the electricity price profile) and storing the energy in the TES for subsequent use during periods of higher fuel/electricity prices.

Fig. 5 shows the duration of the total heat generation, sorted in descending order, for the investigated DH system, as obtained from the modeling. It is clear that the availability of flexibility measures, both TES and DR from the buildings, results in more-stepwise duration curves, although the effect of TES is more pronounced. The plateaus of constant heat generation are noticeably longer in the scenarios with TES, which is attributed to the ability of TES to store heat between seasons, e.g., accumulate excess heat during the summertime and discharge it during the colder months of the year. The modeling results show that mainly due to the availability of TES, the capacity factors of the base-load units (in this work, the source of industrial waste heat and the waste incineration plant) are increased from 0.86 to 0.93 (average values) in the *TES*, *TES*_T_{up} and *TES*_T_{both} scenarios, as compared to the *Ref.* scenario.

The modeling results indicate that the combination of flexibility in the buildings and TES has the greatest effect on the modeled DH system, regarding the operational strategies of the heat generation units. The results show that the total numbers of start-ups of the HPs and electric boilers decrease to the greatest extents, by 78% and 67%, in the *TES*_T_{up} and *TES*_T_{both} scenarios, respectively, as compared to the *Ref.* scenario.

Note that the number of start-ups in the *TES_T$_{both}$* scenario decreases to a lesser extent than in the *TES_T$_{up}$* scenario owing to the high number of substantial, short-term peaks in the space heating demand in buildings, which are distinctive for the *TES_T$_{both}$* scenario (*cf.* Fig. 4b). Furthermore, the numbers of total operational hours of the HPs and electric boilers are also the lowest in the *TES_T$_{up}$* and *TES_T$_{both}$* scenarios: around 40% lower than in the *Ref.* scenario. The number of start-ups and the number of operational hours for the heat generation units for all the investigated scenarios are listed in Appendix C, Tables C1 and C2, respectively.

It is noteworthy that the heat generation and storage capacity mix applied in this work is based on investment modeling applying different assumptions. Thus, the aim is not to project any future development but rather to show the effect of DR in the buildings and the influence of TES on the operational strategies of the DH system. It is worth noting, however, that as long as the DH system consists of heat generation technologies with different characteristics, e.g., running costs, there will be merit order of the technologies and, therefore, there will be value associated with providing flexibility to the system, which can take on even greater prominence if the technologies either consume or produce electricity.

The modeling results indicate that the investigated flexibility measures, in the form of flexible energy use in buildings and a seasonal TES, are economically beneficial and complementary from a systems perspective. Fig. 6 shows the changes in the total yearly system running cost and the total yearly space heating load supplied by the DH system, as obtained from the modeling of the *T$_{up}$*, *T$_{both}$*, *TES*, *TES_T$_{up}$*, *and TES_T$_{both}$* scenarios. The comparison is given in percentages relative to the *Ref.* scenario (100%). The results show that the total system running cost decreases to the greatest extent, i.e., by around 40%, in the scenarios with TES, as compared to the *Ref.* scenario. The total system running cost decreases to a lesser degree in the *T$_{up}$* and *T$_{both}$* scenarios (by around 10%, compared to the *Ref.* scenario). These results indicate that: 1) the studied TES confers greater economic benefits on the DH system, in terms of reduced running cost, than allowing for energy flexibility in the buildings, if comparing their individual effects; and 2) if applied together, energy flexibility in the buildings and the TES are complementary from a systems perspective.

The modeling results show that allowing for upregulation of the indoor temperature has a greater impact on the system (the building stock and DH system) than allowing for downregulation of the indoor temperature. Fig. 6 shows that by allowing only upward temperature regulation in buildings (*T$_{up}$* scenario), the total system running cost decreases by 9%, as compared to the value for the *Ref.* scenario. Whereas, allowing for downregulation of the temperature in addition to upregulation of the temperature in buildings (*T$_{both}$* scenario) affects the system marginally: the total yearly system running cost in the *T$_{both}$* scenario is around 2% lower than that in the *T$_{up}$* scenario (reductions of approximately 11% compared to the *Ref.* scenario). Noticeably, the difference in total system running cost between the *TES_T$_{up}$* and *TES_T$_{both}$* scenarios is also small. Fig. 6 also shows that the total yearly space heating load supplied to the buildings by the DH system is only slightly higher in the *T$_{up}$* and *TES_T$_{up}$* scenarios than in the *Ref.* scenario. This is because the application of active DR results in higher average indoor temperatures in the buildings and, therefore, higher energy losses and a higher space heating load. In the *T$_{both}$* and *TES_T$_{both}$* scenarios, the total yearly space heating loads supplied by the DH system are lower than in the *T$_{up}$* and *TES_T$_{up}$* scenarios, by 2% and 4%, respectively. The reductions in the space heating load achieved through downregulation of the indoor temperature are small, especially in the MFDs and NRBs, as mentioned earlier. This is probably because the periods of allowed downregulation are too short for the buildings to substantially decrease and then restore the temperature with the U-values applied to the buildings. However, it should be noted that the operational energy savings achieved through downregulation of the indoor temperature could have been utilized to a greater extent if investment (capital) costs were included in the EBUC model applied in this work, given that lower demand results in lower investments in generation capacity.

4. Conclusions

The reciprocal effects of the space heating demand flexibility of buildings and operation of DH systems with and without a centralized TES are investigated using a techno-economic, integrated, demand-supply optimization model. The work is based on six investigated scenarios, which differ with respect to the type of flexibility being allowed: (i) demand-side flexibility, achieved by only upward or both upward and downward temperature deviations in buildings; (ii) supply-side flexibility, provided by a TES; and (iii) supply-side and demand-side flexibilities at the same time.

The modeling results reveal that the building type and the availability of a centralized TES in the DH system influence the operational behaviors of the buildings in terms of indoor temperature and space heating demand variations. The results show that the potential to upregulate the indoor temperature (DR) is utilized to a greater extent by the MFDs and NRBs, whereas the potential to downregulate the indoor temperature (operational energy savings) is utilized to a greater extent by the SFDs. This difference is attributed to the fact that the MFDs and NRBs have higher thermal capacities and, therefore, greater potentials for storing the energy. The SFDs, owing to their lighter structures and higher surface area-to-volume ratios, are more suited to exploiting the potential of operational energy savings by reducing the indoor air temperature. We also show that that availability of a TES in the DH system reduces the need for upregulation of the indoor temperature – smoothening of the heat generation is mainly achieved using the TES, and this makes it possible to use more downregulation of the indoor temperature to achieve additional operational energy savings in all the building types.

The modeling results show that allowing for upregulation of the indoor temperature has a stronger impact on the system (building stock and DH system) than allowing for downregulation of the indoor temperature in buildings, i.e., the total system running cost decreases by 9% with only upward temperature deviations being allowed and by 11% with both upward and downward temperature deviations being allowed, when these two scenarios are compared to the Reference scenario. We also show that the studied TES provides greater economic benefits to the DH system, in terms of reduced running cost, than allowing for energy flexibility in the buildings applied individually. However, when applied together, energy flexibility in the buildings and TES are complementary from a systems perspective, i.e., operational energy savings in buildings through reduced temperatures can be achieved.

Declaration of Competing Interest

The authors report no declarations of interest.

Acknowledgments

This work was financed by the E2B2 Research Program and Formas.

Appendix A

Table A1
The EBUC model input parameters used to characterize the investigated building stock and the investigated district heating system of Gothenburg.

Building stock model	
Description	*Units*
Total heated floor area of a building	m^2
Total area of the external surfaces of a building	m^2
Total area of the window surfaces of a building	m^2
Shading coefficient of windows	-
Frame coefficient of windows	-
Coefficient of solar transmission through windows	-
Average U-value of a building	kW/ $m^2.°C$
Thermal mass of the external thermal zone	kWh/°C
Thermal mass of the internal thermal zone	kWh/°C
Solar irradiation	kW/m^2
Outdoor temperature	°C
Average constant values of the heat gains due to: - ventilation fan operation, lighting, electrical appliances and occupants	kW/m^2
Hourly profiles of the heat gains due to:- lighting, electrical appliances and occupants	-
Efficiency of a heat recovery system (if available)	%

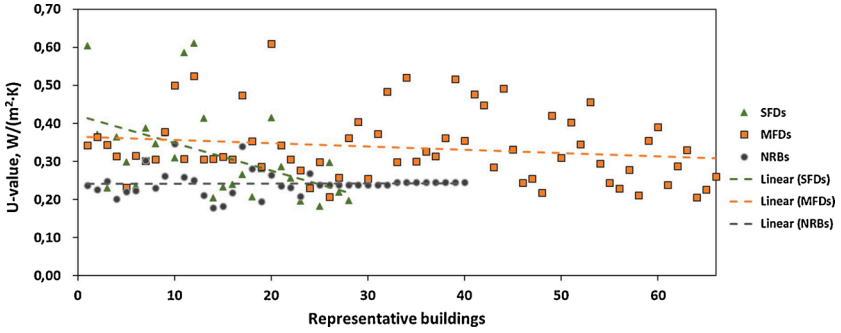

Fig. A1. The U-values of the representative buildings used in this work. SFDs, single-family dwellings; MFDs, multi-family dwellings; NRBs, non-residential buildings.

Table A2
The assumed technical and economic parameters of the heat generation units included in this work.

Heat generation technology	Installed capacity, MW	Minimum generation, MWh/h	Efficiency/COP, %	Ramp rate, MW	Fuel/electricity cost, €/MWh_{fuel}	Variable cost,€/ MWh_{heat}	Energy tax,€/ MWh_{input}
Industrial waste heat[1]	80	40	100	7,5	-	1	-
Waste incineration plant[1]	185	75	100	55	-	1	-
Heat pump, water-based	155	15.5	temperature dependent	-	electricity price	1.7[2]	29[3]
Heat pump, air-based	115	11.5	temperature dependent	-	electricity price	1.7[2]	29[3]
Electric boiler	200	20	99	-	electricity price	0.5[2]	29[3]

[1] The values for the industrial waste heat and waste incineration plant are based on the existing units in the DH system of Gothenburg and are provided by the DH system operator for Year 2012.
[2] The values for variable cost are obtained from the Danish Energy Agency (2016).
[3] The values for the energy tax for Year 2050 are assumed to be the same as for Year 2012 (Nordenergi, 2014).

Table A3
The assumed technical parameters of the pit thermal energy storage unit included in this work.

	Storage capacity, GWh	C-factor	Charging efficiency, %	Discharging efficiency, %	Losses, %	Constant losses, %
Pit TES	77.5	1/210[1]	98[2]	98[2]	0.004[3]	0.017[3]

[1] The value of the C-factor is calculated based on the information for the Sunstore 3 Dronninglund Plant, Denmark (Global Solar Thermal Energy Council, 2019).
[2] The values for the charge/discharge efficiencies are obtained from elsewhere (Romanchenko et al., 2018).
[3] The description and the values of the energy losses from the TES can be found elsewhere (Romanchenko et al., 2020).

Appendix B

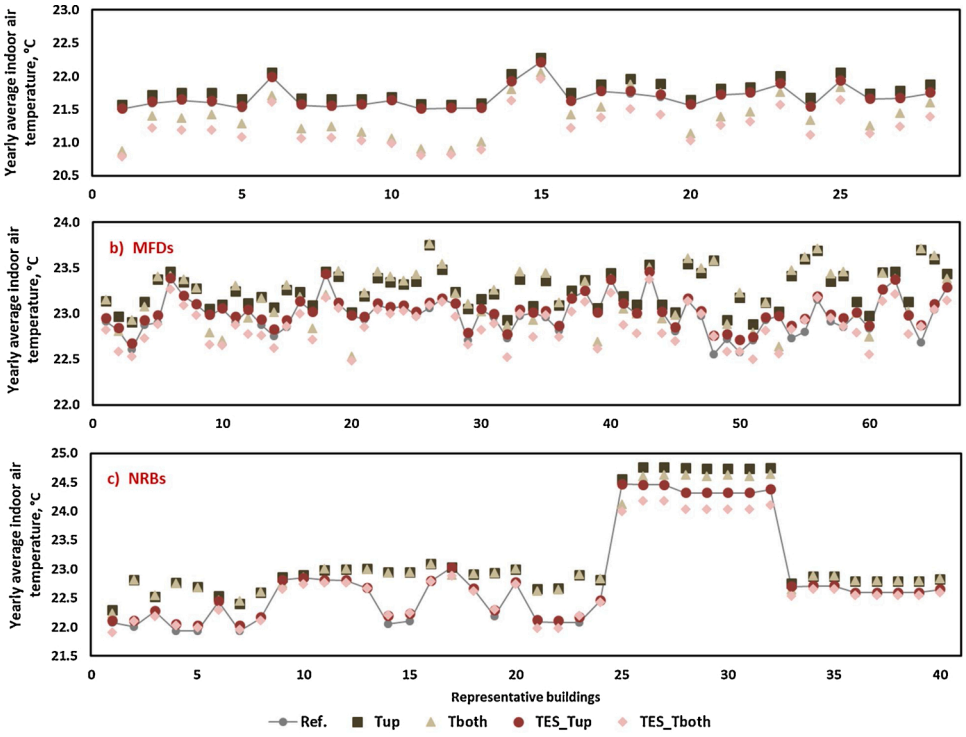

Fig. B1. The yearly (excluding the period from May 15th to September 15th) average indoor air temperatures in the studied SFDs (a), MFDs (b), and NRBs (c), as obtained through the EBUC modeling for the *Ref.*, T_{up}, T_{both}, TES_T_{up}, and TES_T_{both} scenarios (the temperatures in the *TES* scenario are identical to the temperatures in the *Ref.* scenario and, therefore, are not presented). Note that the *y*-axes in a), b), and c) have different bounds. The representative NRBs with the average indoor air temperature at/over 23 °C are the educational NRBs (edNRBs).

Appendix C

Table C1
The numbers of start-ups of the heat generation units in the studied DH system of Gothenburg, obtained through the EBUC modeling for the six investigated scenarios.

Scenarios	Industrial waste heat[1]	Waste incineration plant[1]	Heat pump, water-based	Heat pump, air-based	Electric boiler
Ref.	1	1	128	260	198
DR	1	1	147	116	48
DR_Tdown	1	1	164	145	50
TES	1	1	149	41	7
TES_DR	1	1	105	33	5
TES_DR_Tdown	1	1	142	33	37

[1] The source of the industrial waste heat and the waste incineration plant are assumed to be in operation throughout the whole modeling period, based on the information provided by the DH system operator.

Table C2
The numbers of operational hours of the heat generation units in the studied DH system of Gothenburg, obtained through the EBUC modeling for the six investigated scenarios.

Scenarios	Industrial waste heat[1]	Waste incineration plant[1]	Heat pump, water-based	Heat pump, air-based	Electric boiler
Ref.	8,735	8,735	3,272	1,428	424
DR	8,735	8,735	2,690	968	99
DR_Tdown	8,735	8,735	2,533	942	100
TES	8,735	8,735	2,088	857	204
TES_DR	8,735	8,735	1,941	826	232
TES_DR_Tdown	8,735	8,735	1,847	793	254

[1] The source of the industrial waste heat and the waste incineration plant are assumed to be in operation throughout the whole modeling period, based on the information provided by the DH system operator.

Appendix D. Supplementary data

Supplementary material related to this article can be found, in the online version, at doi:https://doi.org/10.1016/j.scs.2020.102510.

References

Bachmaier, A., Narmsara, S., Eggers, J.-B., & Herkel, S. (2016). Spatial distribution of thermal energy storage systems in urban areas connected to district heating for grid balancing—A techno-economical optimization based on a case study. *Journal of Energy Storage, 8*, 349–357.

Buoro, D., Pinamonti, P., & Reini, M. (2014). Optimization of a Distributed Cogeneration System with solar district heating. *Applied Energy, 124*, 298–308.

Cai, H., Ziras, C., You, S., Li, R., Honore, K., & Bindner, H. W. (2018). Demand side management in urban district heating networks. *Applied Energy, 230*, 506–518.

Danish Energy Agency. (2016). *Technology Data for Energy Plants for Electricity and District heating generation*. Copenhagen: Danish Energy Agency.

Dominković, D., Gianniou, P., Münster, M., Heller, A., & Rode, C. (2018). Utilizing thermal building mass for storage in district heating systems: Combined building level simulations and system level optimization. *Energy, 153*, 949–966.

GAMS.com. (2015). *GAMS Development Corporation, 2015. [Online]. Available: http://www.gams.com/dd/docs/solvers/cplex/#CPLEX_MIXED_INTEGER_PROGRAMMING. [Accessed 26 June 2015]*.

Global Solar Thermal Energy Council. (2019). *"www.solarthermalworld.org"," [Online]. Available: https://www.solarthermalworld.org/news/seasonal-pit-heat-storage-cost-benchmark-30-eurm3. [Accessed 28 10 2019]*.

Göransson, L., Goop, J., Unger, T., Odenberger, M., & Johnsson, F. (2014). Linkages between demand-side management and congestion in the European electricity transmission system. *Energy, 69*, 860–872.

Grundsell, J. (2013). *Bottom-up Description of the Swedish Non-Residential Building Stock—Archetype Buildings and Energy Demand*. Gothenburg: Chalmers ReproService.

GÜNGÖR, G. (2015). *Thermal Comfort and Energy Consumption of A Typical Office Building*. Gothenburg, Sweden: Chalmers University of Technology.

Ingvarson, L. O., & Werner, S. (2008). Building mass used as short term heat storage. In *11th International Symposium on District Heating and Cooling*.

ISO. (2005). *I. 7730:2005, "Ergonomics of the Thermal Environment—Analytical Determination and Interpretation of Thermal Comfort Using Calculation of the PMV and PPD Indices and Local Thermal Comfort Criteria," ISO, Geneva, Switzerland*.

Kensby, J., Trüschel, A., & Dalenbäck, J.-O. (2015). Potential of residential buildings as thermal energy storage in district heating systems – Results from a pilot test. *Applied Energy, 137*, 773–781.

Langer, S., & Bekö, G. (2013). Indoor air quality in the Swedish housing stock and its dependence on building characteristics. *Building and Environment, 69*, 44–54.

Li, H., & Wang, S. J. (2015). Load Management in District Heating Operation. *The 7th International Conference on Applied Energy - ICAE2015*.

Li, Y., Rezgui, Y., & Kubicki, S. (2020). An intelligent semantic system for real-time demand response management of a thermal grid. *Sustainable Cities and Society, 52*.

Lund, P. D., Lindgren, J., Mikkola, J., & Salpakari, J. (2015). Review of energy system flexibility measures to enable high levels of variable renewable electricity. *Renewable and Sustainable Energy Reviews, 45*, 785–807.

Nordenergi, W. G. (2014). *Nordic Tax Report 2013 - Electricity Sector*. WG: Nordenergi.

Odenberger, M., Unger, T., & Johnsson, F. (2009). Pathways for the North European electricity supply. *Energy Policy, 37*(no. 5), 1660–1677.

Oluleye, G., Vasquez, L., Smith, R., & Jobson, M. (2016). A multi-period Mixed Integer Linear Program for design of residential distributed energy centres with thermal demand data discretisation. *Sustainable Production and Consumption, 5*, 16–28.

Paiho, S., Saastamoinen, H., Hakkarainen, E., Similä, L., Pasonen, R., Ikäheimo, J., Rämä, M., Tuovinen, M., & Horsmanheimo, S. (2018). Increasing flexibility of Finnish energy systems—A review of potential technologies and means. *Sustainable Cities and Society, 43*, 509–523.

Romanchenko, D., Odenberger, M., Göransson, L., & Johnsson, F. (2017). Impact of electricity price fluctuations on the operation of district heating systems: A case study of district heating in Göteborg, Sweden. *Applied Energy, 204*, 16–30.

Romanchenko, D., Kensby, J., Odenberger, M., & Johnsson, F. (2018). Thermal energy storage in district heating: Centralised storage vs. storage in thermal inertia of buildings. *Energy Conversion and Management, 162*, 26–38.

Romanchenko, D., Nyholm, E., Odenberger, M., & Johnsson, F. (2019). Flexibility Potential of Space Heating Demand Response in Buildings for District Heating Systems. *Energies, 12*.

Romanchenko, D., Nyholm, E., Odenberger, M., & Johnsson, F. (2020). *Balancing investments in building energy conservation measures with investments in district heating – A Swedish case study," To be submitted.*.

SMHI—Swedish Meteorological and Hydrological Institute. (2017). *http://strang.smhi.se/," [Online]. Available: http://strang.smhi.se/extraction/index.php. [Accessed 24 11 2017]*.

Socialstyrelsen. (2005). *Temperatur inomhus*. Lindesberg: Bergslagens Grafiska.

The National Board of Housing, B. a. P. (2010). *Teknisk Status i den Svenska Bebyggelsen - Resultat Från Projektet BETSI*. Karlskrona, Sweden: Boverket.

Verrilli, F., Srinivasan, S., Gambino, G., Canelli, M., Himanka, M., Vecchio, C. D., Sasso, M., & Glielmo, L. (2017). Model Predictive Control-Based Optimal Operations of District Heating System With Thermal Energy Storage and Flexible Loads. *IEEE TRANSACTIONS ON AUTOMATION SCIENCE AND ENGINEERING*.